On the Trochoidal motion model of a sensor placed off-centered inside a rolling ball

Fabian Arzberger[1], Fabian Wiecha[1], Jasper Zevering[1], Julian Rothe[2], Dorit Borrmann[3], Sergio Montenegro[2], and Andreas Nüchter[1]

Abstract— **We study the motion model of a sensor rigidly mounted inside a ball, with the extrinsic parameters of the sensor with respect to the balls center of rotation being known by calibration. Due to the rigid placement inside the ball, the geometry of the sensors trajectory resembles a 3D-Trochoid. The motion model, which encorporates angular velocities, the radius of the ball, and the ground normal, estimates the full 6-DoF pose of the sensor and is used in an extended Kalman-filter. We deploy this motion model on our sherical mobile mapping platform to estimate the trajectory of a LiDAR sensor. The evaluation shows that this approach improves the mapping accuracy, compared to our previous method which did not use a Kalman filter, and also compared to a more simple non-Trochoidal motion model using the Kalman-filter.**

I. Introduction

II. Related work

III. Extrinsic calibration

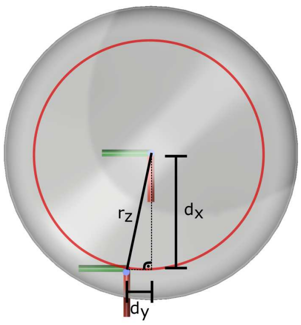

Fig. 1: Calibration principle of a sensor inside a ball, illustrated in one axis.

The sensor, when mounted off-centered in the ball, will make circular trajectories if the ball rotates around an axis through its center. We measure the radii of the sensor around the three orthogonal principal axes, which is enough information to construct the extrinsic parameters, describing the offset to the balls center.

IV. Trochoidal motion model

The sensors rotation around the balls center is described through the rotation derivative which correspond to local gyro measurements $\vec{\omega}^r$

$$\frac{d}{dt}\mathbf{R}_r = \vec{\omega}^r_\times \cdot \mathbf{R}_r \quad , \tag{1}$$

where the cross-product matrix is defined as

$$\vec{\omega}_\times = \begin{pmatrix} 0 & -\omega_3 & \omega_2 \\ \omega_3 & 0 & -\omega_1 \\ -\omega_2 & \omega_1 & 0 \end{pmatrix} \quad . \tag{2}$$

Go study group theory and learn about the Lie algebra $\mathfrak{so}(3)$ which is the tangent space to $\mathrm{SO}(3)$ at its identity, to find out why this works. Anyways, through the inverse rotation we transform the local measurements into the global frame, leading to

$$\vec{\omega} = \mathbf{R}_r^{-1} \cdot \vec{\omega}^r \tag{3}$$

and

$$\vec{s} = \mathbf{R}_r^{-1} \cdot \vec{s}^r + \vec{p} \tag{4}$$

with

$$\vec{p}(t) = \int_0^t \vec{v}(\tau)d\tau \quad , \tag{5}$$

where the velocity of the balls center over ground with normal $\vec{n}$ is

$$\vec{v} = r_s \vec{\omega} \times \vec{n} \quad . \tag{6}$$

The combined model:

$$\vec{s} = \mathbf{R}_r^{-1} \cdot \vec{s}^r + \int \left(\left[\mathbf{R}_r^{-1} \cdot r_s \cdot \vec{\omega}^r \right] \times \vec{n} \right) \tag{7}$$

expands, not ommiting the time dependence, to:

$$\vec{s}(t) = \left[\int_0^t \vec{\omega}^r_\times(\tau)\mathbf{R}_r(\tau)d\tau \right]^{-1} \vec{s}^r + \int_0^t \left(\left[\left\{ \int_0^t \vec{\omega}^r_\times(\tau)\mathbf{R}_r(\tau)d\tau \right\}^{-1} r_s \vec{\omega}^r(\tau) \right] \times \vec{n}(\tau) \right) d\tau \tag{8}$$

which is the kinematic model to be solved numerically for any arbitrary gyro measurements.

*We acknowledge funding from the ESA Contract No. 4000130925/20/NL/GLC for the study “DAEDALUS – Descent And Exploration in Deep Autonomy of Lava Underground Structures” within the Open Space Innovation Platform (OSIP) lunar caves-system and the Elite Network Bavaria (ENB) for providing funds for the academic program “Satellite Technology”

[1]The authors are with Computer Science XVII – Robotics, Julius-Maximilians-Universität Würzburg, 97074 Am Hubland, Germany. Contact: `fabian.arzberger@uni-wuerzburg.de`

[2]The authors are with Computer Science VIII – Aerospace Information Technology, Julius-Maximilians-Universität Würzburg, 97074 Am Hubland, Germany. Contact: `julian.rothe@uni-wuerzburg.de`

[3]Dorit Borrmann is with THWS Robotics, Technische-Hochschule-Würzburg-Schweinfurt, 97421 Schweinfurt, Germany. Contact: `dorit.borrmann@thws.de`

979-8-3503-0704-723$31.00 ©2023 IEEE

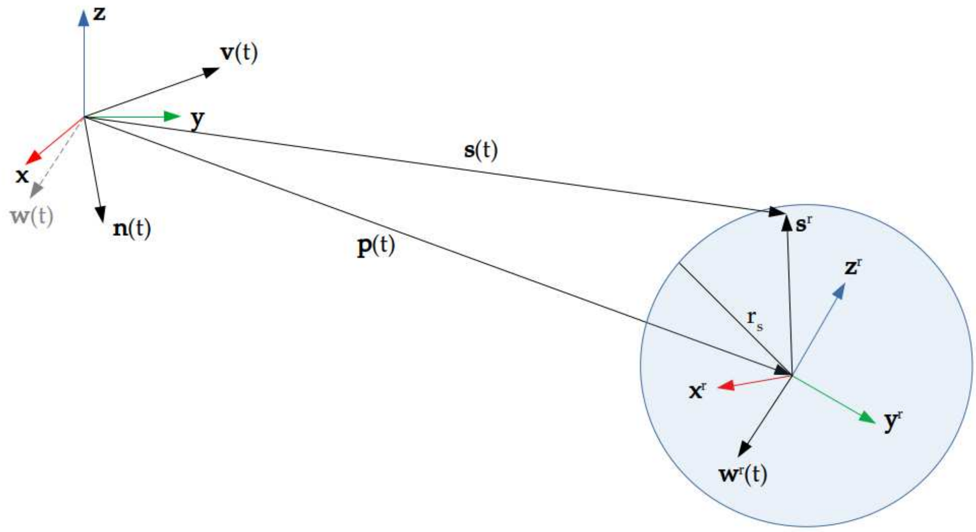

Fig. 2: Schematics of the motion model

V. Extended Kalman filter

VI. Implementation

VII. Experimental evaluation

A. Trajectories

B. 3D Point Clouds

VIII. Conclusions